# Proof Delivery Form

**Journal and Article number:** BCJ-2017-0189

**Number of pages (not including this page):** 12

---

## Biochemical Journal

**Please check your proof carefully to ensure (a) accuracy of the content and (b) that no errors have been introduced during the production process.**

- You are responsible for ensuring that any errors contained in this proof are marked for correction before publication. Errors not marked may appear in the published paper.
- Corrections should only be for typographical errors in the text or errors in the artwork; substantial revision of the substance of the text is not permitted.
- Please answer any queries listed below.
- If corrections are required to a figure, please supply a new copy.

Your proof corrections and query answers should be returned as soon as possible (ideally within 48 hours of receipt). Please upload your corrected proof and any additional files (e.g. artwork) via the online proof review page from which you downloaded this file. You can also provide any specific instructions or comments in the 'Response Comments' box on the online page.

*Notes:*

1. Please provide the paper's reference number in any correspondence about your article
2. If you have any queries, please contact the publisher by email (production@portlandpress.com) or by telephone +44 (0)20 7685 2410

---

## Supplementary Material:

This proof does not contain any supplementary material. If supplementary content is associated with this article it will be published, in the format supplied by the authors, with the online version of the article.

---

## Queries for author:

Q1: Please verify that the edit retains your intended meaning, as your original sentence was unclear.

Q2: References [26–40] have been renumbered because they were cited out of order. Please check that the renumbered references are correct in the text and reference list.

Q3: Please check ref. citation not in order.

Q4: Please revise 'and between them', as the meaning is unclear in this sentence.

Q5: Does any information here constitute a potential competing/conflict of interest? If so, please move to the Competing Interests section.

Q6: Please confirm that all sources of funding (including all relevant grant numbers) have been acknowledged in Funding section.

Q7: Please confirm that this statement is an accurate reflection of any competing interests (or lack thereof) of the author(s).

Q8: Please confirm if this statement is correct.

Q9: Please provide main title for Figure 1.

Q10: The following terms have been used in this figure: Abs, A.U. If any of these are abbreviations that can be defined, and whose definition would be beneficial to readers, please add these to the figure caption.

*Biochemical Journal* (2017) **0** 1–12
DOI: 10.1042/BCJ20170189

PORTLAND PRESS

Research Article

# Characterization of the oligomeric states of the CK2 $\alpha_2\beta_2$ holoenzyme in solution

**Graziano Lolli[1,3], Denise Naressi[1], Stefania Sarno[2] and Roberto Battistutta[1]**

[1]Department of Chemical Sciences, University of Padua, via Marzolo 1, Padova 35131, Italy; [2]Department of Biomedical Sciences, University of Padua, Via Ugo Bassi 58/B, Padova 35121, Italy; and [3]Present address: CIBIO, Centre for Integrative Biology, University of Trento, via Sommarive 9, Povo 38123, Italy

Correspondence: Roberto Battistutta (roberto.battistutta@unipd.it) or Graziano Lolli (graziano.lolli@unitn.it)

The regulatory mechanism of protein kinase CK2 has still to be fully clarified. The prevailing hypothesis is that CK2 is controlled by a self-polymerisation mechanism leading to inactive supramolecular assemblies that, when needed, can be disassembled into the $\alpha_2\beta_2$ monomer, the active form of the holoenzyme. *In vitro*, monomeric $\alpha_2\beta_2$ seems present only at high ionic strengths, typically 0.35–0.50 M NaCl, while at lower salt concentrations oligomers are formed. In the present study, size-exclusion chromatography (SEC), dynamic light scattering (DLS), small-angle X-ray scattering (SAXS) and mutagenesis have been employed for the characterization of the oligomeric states of CK2 in solution. SAXS measurements at 0.35 M NaCl show for the first time the shape of the $\alpha_2\beta_2$ active monomer in solution. At 0.25 M salt, despite single average properties indicating an aggregated holoenzyme, deconvolution analysis of SAXS data reveals an equilibrium involving not only circular trimeric and linear oligomeric (3–4 units) forms of $\alpha_2\beta_2$, but also considerable amounts of the monomer. Together SAXS and mutagenesis confirm the presence in solution of the oligomers deduced by crystal structures. The lack of intermediate species such as $\alpha\beta_2$, $\alpha$ or $\beta_2$ indicates that the holoenzyme is a strong complex that does not spontaneously dissociate, challenging what was recently proposed on the basis of mass spectrometry data. A significant novel finding is that a considerable amount of monomer, the active form of CK2, is present also at low salt. The solution properties of CK2 shown in the present study complement the model of regulation by polymerization.

## Introduction

CK2 is a highly pleiotropic and conserved Ser/Thr protein kinase that is involved in many cellular processes such as gene expression, cell cycle progression, embryogenesis, cell growth and differentiation, circadian rhythms and apoptosis [1]. Deregulation of the CK2 catalytic activity has been linked to several pathologies, mainly cancers, but also neurodegenerative disorders such as Alzheimer's disease, Parkinson's disease and amyotrophic lateral sclerosis, inflammation and cardiovascular diseases. The oncogenic potential of CK2 mainly relies on the capacity to act as an anti-apoptotic agent [2] and has been connected to abnormally high levels of the enzymatic activity found in a large variety of solid and haematological tumours [3]. Nowadays CK2 is considered a validated drug target, with two inhibitors in ongoing clinical trials as antitumor agents [4–9].

The regulatory mechanism of the CK2 catalytic activity has not been fully elucidated yet. CK2 is not regulated by 'conventional' mechanisms common to other eukaryotic protein kinases, such as phosphorylation or dephosphorylation events, second messenger binding or reversible association with regulatory subunits, with the consequence that its catalytic domain is not shifting between inactive and active conformations. Indeed CK2 is often referred to as 'constitutively active', as its catalytic $\alpha$ subunit has been always found in an active state in the many crystal structures determined so far, with all the structural elements necessary for catalysis locked in the proper position by structural

Received: 9 March 2017
Revised: 29 May 2017
Accepted: 1 June 2017

Accepted Manuscript online: 1 June 2017
Version of Record published: 0 Month 2017

Biochemical Journal (2017) 0 1–12
DOI: 10.1042/BCJ20170189

features peculiar to CK2 [10–12]. The binding of the so-called 'regulatory' β subunit to form the tetrameric $\alpha_2\beta_2$ holoenzyme leaves the structure of the catalytic subunit substantially unaffected in its main features, so that both the holoenzyme and the isolated α-subunit are catalytically active, although to a different extent depending on substrates. Apart from different expression or localization issues of the two subunits, *in vivo* the fully functional form of CK2 is considered to be the $\alpha_2\beta_2$ holoenzyme, a heterocomplex of 140 kDa. Besides those of the isolated α- and β-subunits, several crystal structures of the holoenzyme are now available [13–16]; the constitutive $\beta_2$ dimer recruits two α-subunits on opposite sides, originating a 'butterfly'-shaped, prolate heterocomplex in which the two catalytic subunits do not interact with each other.

Based on self-aggregation properties leading to filaments of *Drosophila* CK2, in 1986 Claiborne V. C. Glover proposed that this enzyme could be unconventionally regulated by an oligomerization process, with the formation of inactive regular aggregates that could constitute the functional state of this kinase at rest [17,18]. Activity is restored by (as yet unknown) events that trigger the dissociation of oligomers into the monomeric, active form of the tetrameric holoenzyme. Currently this mechanism is the most accepted working model for CK2 and has been supported over time by *in vitro* and *in vivo* studies [19–22].

Crystal structures of the holoenzyme have supported this model of regulation suggesting how CK2 can oligomerize via the formation of circular trimers (PDB IDs 1JWH [13] and 4DGL [14]) and linear oligomers (PDB IDs 4MD7, 4MD8, 4MD9 [15] and 4NH1 [16]) (Figure 1). In both cases aggregation is driven by intermolecular electrostatic interactions involving the basic P + 1 loop of the α-subunit and the so-called 'acidic loop' of the β-subunit of another holoenzyme. By means of mutagenesis studies these two regions were previously seen as directly implicated in the regulation of the catalytic activity [23,24], but, due to the lack of the crystal structure of the holoenzyme at that time, these inhibitory 'secondary interactions' were wrongly interpreted as intra-tetrameric, i.e. among subunits of the same $\alpha_2\beta_2$ assembly.

The significance of the oligomeric forms deduced from crystal packings of the CK2 holoenzyme needs to be substantiated by a structural characterization that provides evidences of their existence and stability in solution. Very recently, the ionic-strength dependent oligomerization of CK2 has been analysed by native mass spectrometry, bringing evidence of the existence of both circular trimers and linear assemblies [25]. The presence of intermediate species of the holoenzyme such as $(\alpha\beta_2)_n$ has been reported as well, leading to the suggestion of the transient nature of the α/β interaction. In the present study, we report solution structure studies by size-exclusion chromatography (SEC), dynamic light scattering (DLS) and small-angle X-ray scattering (SAXS), as well as mutational studies, that further support the presence in solution of the oligomeric species proposed by the crystal structures. In particular, SAXS measurements performed at different salt concentrations (0.35, 0.25 and 0.20 M NaCl) have enabled insights into the equilibria between different oligomeric species, leading to different conclusions regarding the stability of the holoenzyme and the existence of intermediate species in solution.

# Materials and methods

## Sample preparation

For SEC and DLS analyses, the CK2 holoenzyme was produced as detailed in Lolli et al. [14]. For SAXS experiments, CK2α and CK2β were first produced and purified to homogeneity separately and then used to reconstitute the $\alpha_2\beta_2$ holoenzyme. CK2α (aa. 1–336, called $CK2\alpha^{(1-336)}$) was produced as previously reported [6]. CK2β was produced in *Escherichia coli* at 30°C by induction with 0.5 mM IPTG for 4 h and purified by a three-step purification protocol using HiTrap Heparin (GE Healthcare), MonoQ (GE Healthcare) and Superdex 75 (GE Healthcare) columns, as detailed in the Supplementary material. The $\alpha_2\beta_2$ holoenzyme was reconstituted by mixing CK2α and the CK2β dimer in a ratio 4:1; the excess of CK2α was removed by SEC on a Superdex 200 column (GE Healthcare) using 25 mM Tris pH 8.5, 0.35 M NaCl and 0.2 mM TCEP as running buffer. The MW of the $\alpha_2\beta_2$ holoenzyme under investigation, carrying the C-terminal truncated $CK2\alpha^{(1-336)}$, was 130 kDa versus 140 kDa for the holoenzyme with full-length α. CK2 mutants were produced according to Boldyreff et al. [23] and Sarno et al. [24].

## SEC and DLS analyses

Chromatographic runs were performed on an ÄKTApurifier 10 system (GE Healthcare) equipped with a UV-visible detector set at 280 nm. Superdex 200 10/300 (GE Healthcare) and Superose 6 10/300 (GE Healthcare) were calibrated using the HMW calibration kit (GE Healthcare) and following the manufacturer's

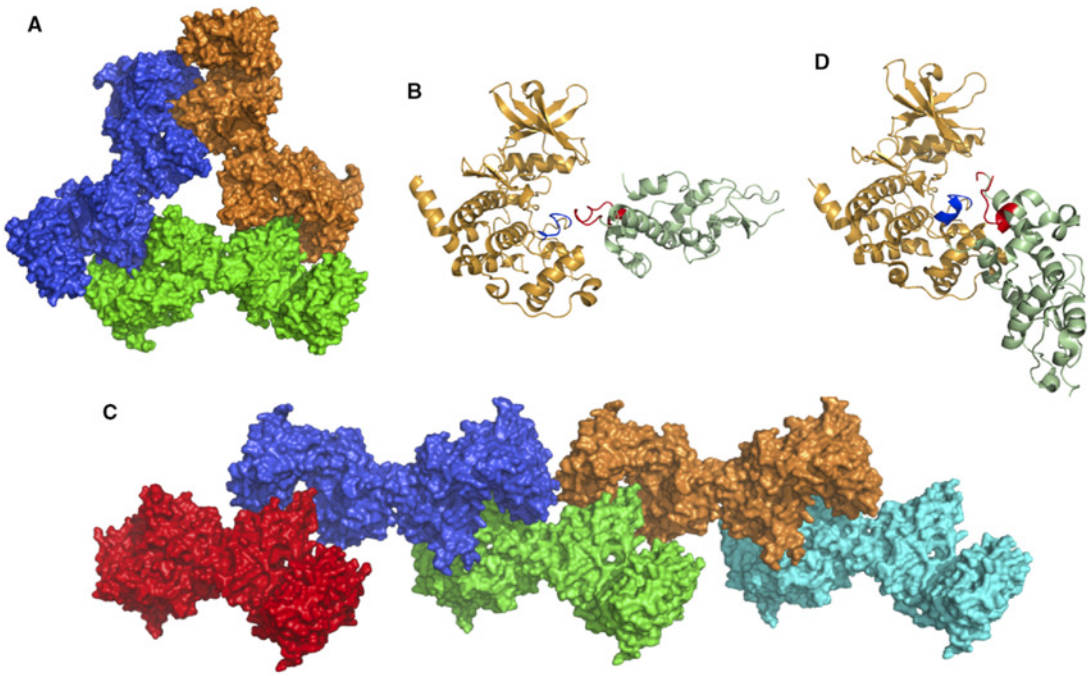


**Figure 1.** Architecture of the circular trimer (**A**, viewed along the three-fold symmetry axis) and linear oligomers (**C**, a linear pentamer in this case) of the CK2 holoenzyme, based on the PDB IDs 4DGL (hexagonal form with asymmetric $\alpha_2\beta_2$) and 4MD7 (monoclinic form with symmetric $\alpha_2\beta_2$), respectively. Single $\alpha_2\beta_2$ monomeric assemblies have different colours. Different inter-molecular orientation between the α-subunit of one monomer (orange) and the β-subunit of the neighbouring monomer (green) in the circular trimer and in the linear oligomers are shown in panels **B** and **D**, respectively. In both cases, electrostatic interactions between the basic P + 1 loop of the α-subunit (blue) and the 'acidic loop' of the β-subunit (red) are involved, even though with a different arrangement.

Q9

instructions (Supplementary Figure S1). CK2 holoenzyme (2 mg/ml, 25 µl) was loaded on the pre-equilibrated columns and eluted with buffers composed of 25 mM Tris pH 8.5, TCEP 0.2 mM and NaCl concentrations ranging from 0.5 to 0.15 M, at a constant 0.5 ml/min flow rate. For DLS analyses, the CK2 holoenzyme was tested at 5 mg/ml in the above buffer at 25°C, with either 0.5 or 0.25 M NaCl, by using a Zetasizer Nano™ (Malvern Instruments). Samples were centrifuged at 12 000 rpm (15 500×***g***, on a Beckman Coulter TA-14-50 rotor) at 4°C for 10 min prior to data collections.

## Small angle X-ray scattering data collection

For the structural characterization of the CK2 holoenzyme in solution SAXS data were collected at the Q2 European Synchrotron Radiation Facility (ESRF) BM29 BioSAXS beamline [26], in the SEC-SAXS mode, with Q3 a SEC column coupled to SAXS measurements [27]. A 100 µl volume of $\alpha_2\beta_2$ at 10 mg/ml in 25 mM Tris pH 8.5, TCEP 0.2 mM and different NaCl concentrations were loaded onto a Superdex 200 10/300 size-exclusion column (GE Healthcare), extensively equilibrated in the same buffering system, in three independent runs differing for the salt concentration, 0.35 M, 0.25 M and 0.20 M NaCl, respectively, at a flow rate of 0.5 ml/min, using the beamline Shimadzu HPLC system. Solution eluting from the column was redirected to the sample flow path for immediate SAXS data collection. Scattering data were collected using a Pilatus 1 M 2D detector from Dectris (detector distance 2.8720 m), corresponding to a momentum transfer s ($4\pi\sin\theta/\lambda$) range of 0.08–4.5 $nm^{-1}$, with 2 s exposure time per frame (approximately 2000 frames were collected per sample run), wavelength 0.99190 Å and temperature 293 K. Initial data processing was performed automatically using the pipeline for bioSAXS data implemented at the ESRF BM29 beamline using the EDNA framework [28] and analysed with the laboratory-information management system ISPyB [29]. Frames 1–749, 1–671 and 1–562 were automatically averaged by the pipeline to yield an 'average buffer' profile for the 0.35 M, 0.25 M and 0.20 M NaCl run, respectively. The 'average buffer' was then subtracted from all frames classified as 'sample' [28]. For

Biochemical Journal (2017) 0 1–12
DOI: 10.1042/BCJ20170189

each of the 0.35 and 0.25 M NaCl runs, two subsets of frames from the peak scattering intensity (one from the front and one from the tail) were selected and manually merged to yield a single averaged frame, according to the invariance of the values for the radius of gyration ($R_G$), the parameter $Q_R$ [30] and the molecular mass. For 0.35 M salt, ranges 816–839 (front) and 888–896 (tail) were selected; for 0.25 M salt, ranges 696–709 (front) and 768–782 (tail) were selected. Single averaged frames were used for all further data processing and model fitting. Manual processing was performed with PRIMUS [31] from the ATSAS 2.7.2 program package [32]. Useful experimental data ranges were determined with SHANUM [33], discarding data at higher angles containing no useful information. Fittings of the experimental scattering profiles with the theoretical ones calculated from known crystal structures (PDB ID 4DGL and 4MD7) were performed with CRYSOL [34] for a single-component mixture and OLIGOMER [31] for a multi-component mixture. *Ab initio* solution reconstruction of the protein shape at 0.35 M NaCl was obtained by GASBOR [35].

# Results

## SEC and DLS results are compatible with the existence of CK2 trimers of tetramers in solution

In a previous study we reported that the CK2 holoenzyme forms circular trimers of tetramers in hexagonal crystals mainly through ionic interactions (Figure 1) [14]. In solution, this species has largely escaped attention due to the established purification protocol for the CK2 holoenzyme, which ensures high yield while keeping the proteins in a high ionic strength environment, typically 0.5 M NaCl, to limit aggregation. In this condition (0.5 M NaCl) our analytical SEC on a calibrated column indicates that CK2 is in the monomeric $\alpha_2\beta_2$ form (Figure 2A). At lower ionic strengths, different oligomeric $(\alpha_2\beta_2)_n$ species of the holoenzyme do appear, the one at 0.25 M NaCl corresponding to a trimeric assembly $(\alpha_2\beta_2)_3$. By lowering further the salt concentration to 0.2 M and 0.15 M the formation of higher-order oligomers with a mean MW of approximately 900–970 kDa is observed.

A similar trend was observed by DLS analyses (Supplementary Figure S2). At 0.5 M NaCl the sample appears to be monodisperse (100% in intensity and volume) with a low polydispersity index 7.9%, a Z-average diameter 11.85 nm and a Stokes radius ($R_S$) 5.93 nm. This value for $R_S$ is higher than that predicted for a globular-shaped protein of 130 kDa (4.77 nm), as expected for a prolate-shaped object as $\alpha_2\beta_2$, a $15.0 \times 7.0 \times 7.0$ nm ellipsoid with an axial ratio of 2.14. At 0.25 M NaCl there are two peaks in intensity, one corresponding to particles with 16.39 nm diameter (97.2% in volume, $R_S$ 8.20 nm) and the other corresponding to very large particles with mean diameter 1124 nm. The smaller particles have an Rs value close to that of a globular-shaped $\alpha_2\beta_2$ trimer (MW 390 kDa, Rs 7.62 nm; for a globular dimer of 260 kDa the theoretical Rs is 6.41 nm), somehow higher in accordance with the elongated shape of both circular trimers ($19.0 \times 19.0 \times 7.0$ nm, oblate shape, axial ratio 2.71) and linear trimers ($30.0 \times 11.5 \times 11.5$ nm, prolate shape, axial ratio 2.60).

## Oligomerization in solution is driven by electrostatic interactions between the CK2α P + 1 loop and the CK2β acidic loop

In both circular trimers (from hexagonal crystals with asymmetric $\alpha_2\beta_2$) and linear oligomers (from monoclinic crystals with symmetric $\alpha_2\beta_2$) the most relevant interaction involves the basic P + 1 loop (Arg191–Lys198) of CK2α and the CK2β acidic loop (Asp55–Asp64) [14–16]. Polyamines are known activators of CK2 [36], the most effective being spermine, supposed to exert their function through interaction with the CK2β acidic loop. We tested by SEC whether spermine is able to interfere with the salt-dependent oligomerization of the CK2 holoenzyme, showing that 5 mM spermine can destabilize oligomeric species of CK2 tetramers in a low ionic strength environment (Supplementary Figure S3). At 0.25 M NaCl, CK2 appears to be mostly monomeric in the presence of spermine (Supplementary Figure S3A); at 0.2 M NaCl, spermine strongly destabilizes the high-molecular-weight aggregated forms observed in its absence (Supplementary Figure S3B). We propose that spermine is able to compete with the basic stretch of CK2α for the inter-molecular binding to the CK2β acidic loop, hampering oligomerization.

To further define the molecular determinants responsible for the oligomerization properties of CK2 we studied a CK2α with residues Arg191, Arg195 and Lys198 mutated to Ala, named α(nobasic), and a CK2β with residues Asp55, Leu56, Glu57 mutated to Ala, named β(noacid). These mutants were already characterized in their catalytic properties by Sarno et al. [24] and by Boldyreff et al. [23], respectively. The interest in these mutants relies on the fact that the mutated residues are those showing the most relevant contacts responsible

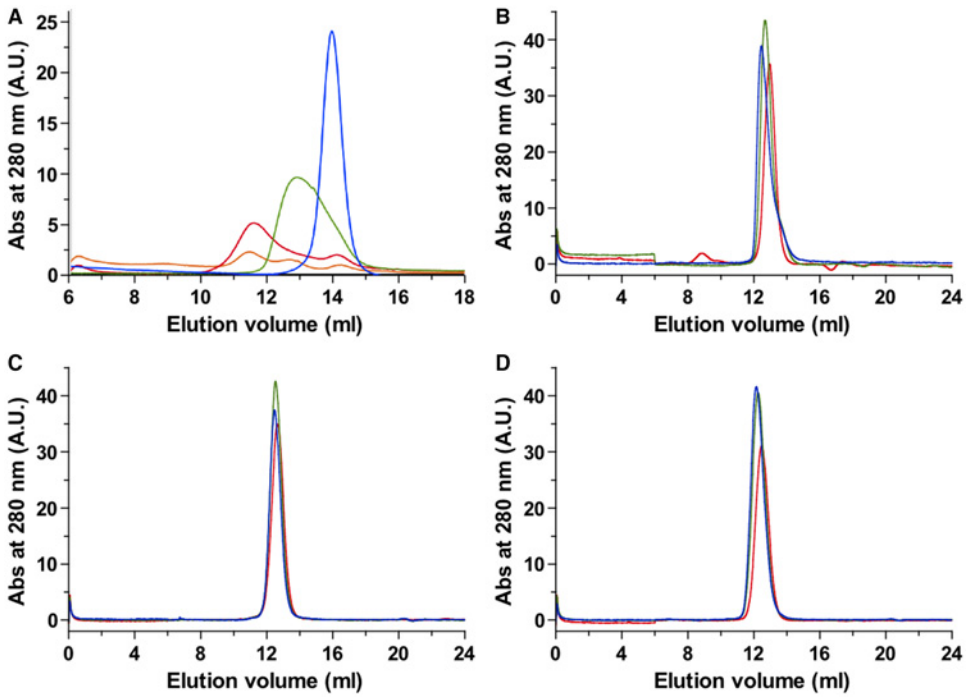


**Figure 2. SEC elution profiles at different NaCl concentrations.**

(**A**) Wild-type $\alpha_2\beta_2$ at 0.50 M (blue), 0.25 M (green), 0.20 M (red) and 0.15 M (orange) NaCl, eluted from a Superpose 6 10/300 GL column. On the basis of column calibration (Supplementary Figure S1), the four main peaks in panel **A** correspond to a monomer at 0.50 M salt, to a trimer at 0.25 M salt (calculated MW 370 kDa) and to higher-order aggregates at 0.20 M and 0.15 M salt (calculated MW 900–970 kDa). The MW of the monomeric holoenzyme was estimated to be 180 kDa in a Superdex 200 column run at 0.50 M NaCl (Supplementary Figure S3, blue profile) on the basis of a calibration at the same salt concentration (Supplementary Figure S1). The difference between the apparent MW of 180 kDa and the theoretical MW can be attributed to the elongated rod-like 'butterfly' shape of the monomer. (**B–D**) elution profiles of CK2 mutants on a Superdex 200 10/300 GL column (red 0.50 M, green 0.25 M and blue 0.20 M NaCl). All peaks correspond to monomeric forms of the holoenzyme, indicating that mutations in either the β-acid loop (**B**) or the α-basic cluster (**C**) are sufficient to abrogate the salt-dependant oligomerization of the wild-type holoenzyme. (**D**) Effect of mutating both the β-acid loop and the α-basic cluster. Elution profiles in panels **B–D** suggests that their dependence on salt concentration for the monomeric CK2 holoenzyme is rather modest.

Q10

for the oligomerization of the holoenzyme as deduced by the crystallographic structures describing circular trimers and linear oligomers. Different CK2 holoenzymes were prepared, by combining the two mutants with the wild-type partners [CK2α(nobasic)/wtCK2β and wtCK2α/CK2β(noacid)] and between them [CK2α (nobasic)/CK2β(noacid)]. According to SEC, none of them was able to form trimers of tetramers or higher-order oligomers at 0.25 M and 0.20 M NaCl, respectively (Figure 2B–D), indicating that the mutated residues are necessary for the oligomerization process.

Q4

## SAXS measurements in solution

For a more detailed characterization of the oligomeric forms of the CK2 holoenzyme in solution, we performed SAXS experiments at different ionic strengths. SAXS data were expected to complement SEC and DLS measurements and to give more detailed information on the size and shape of the species in solution, as well as on their possible equilibria; they could enable recognizing circular trimers and linear oligomers and distinguishing between them.

To obtain the best possible SAXS data we prepared the CK2 tetrameric holoenzyme very carefully. The α- and the β-subunits were produced and purified to homogeneity independently (see the Materials and methods section). For the preparation of $\alpha_2\beta_2$, appropriate aliquots of the single subunits were mixed together and

Biochemical Journal (2017) 0 1–12
DOI: 10.1042/BCJ20170189

loaded on a SEC column equilibrated with 0.35 M NaCl; only fractions corresponding to the full tetrameric holoenzyme were collected for successive SAXS experiments, discarding those at higher elution times. Moreover, diffraction experiments were performed in the SEC-SAXS mode, i.e. with a further SEC run coupled to SAXS measurements, at BioSAXS beamline BM29 of the ESRF. CK2 was analysed at three different salt concentrations, 0.35, 0.25 and 0.2 M NaCl.

At 0.35 M NaCl, CK2 eluted with an asymmetric peak, indicating the presence of some heterogeneity in solution (Supplementary Figure S4). We then decided to analyse two sets of frames, one from the front and one from the tail of the elution peak. The SAXS data on the tail indicate a MW of 128.9 kDa and a radius of gyration of 51.7 Å (Table 1), in accordance with the presence of the monomeric holoenzyme $\alpha_2\beta_2$ (theoretical MW and $R_G$ 130 kDa and 46.87 Å, respectively). The experimental scattering data $I_{exp}$ and the predicted scattering profile $I_{calc}$ for the known atomic structure of the $\alpha_2\beta_2$ monomeric form of the holoenzyme (PDB ID 4DGL) showed good accordance (Figure 3) with a rather low $\chi^2$ of 0.80, as calculated with CRYSOL. For comparison, the fitting using a dimeric holoenzyme is rather poor, with a higher $\chi^2$ of 7.19 (Supplementary Table S1). The comparison between the radius of gyration $R_G$ determined by SAXS and the Stokes radius (known also as hydrodynamic radius) $R_S$ determined by DLS can give useful indications whether a molecule has a spherical or elongated shape. The typical $R_G/R_S$ ratio for a spherical protein is ≈0.775 and tends to higher values for elongated structures. Correspondingly, the $R_G/R_S$ for CK2 at high salt is 0.87, in accordance with the prolate shape of $\alpha_2\beta_2$ and with what was previously derived by DLS alone.

To evaluate the possible presence of other species in solution, in particular of dissociated forms of the holoenzyme, we analysed the scattering data with OLIGOMER, using as input the theoretical scattering profiles of four different atomic models: $\alpha_2\beta_2$, $\alpha\beta_2$ and the isolated α and $\beta_2$. As shown in Supplementary Table S1, none of the dissociated forms of the holoenzyme, neither $\alpha\beta_2$ nor the isolated α and $\beta_2$, are detectable. This reveals that the equilibrium between the single components and the fully formed holoenzyme is largely shifted toward the latter.

The deviation from the linearity of the Guinier plot at very low diffraction angles suggests the presence of some aggregates; we then run OLIGOMER with different combinations of the monomer and possible oligomeric species, the dimer (lDim), the circular trimer (cTri) and the linear trimer (lTri). As reported in Table 1 and Supplementary Table S1, this analysis confirms the presence of some oligomeric forms, but with the dominant presence of the monomeric holoenzyme, approximately 95% in volume.

To evaluate the shape of the scattering object in solution, we used GASBOR, an *ab initio* program that, by means of a simulated annealing protocol, is able to obtain a structural model from X-ray solution scattering data using a spatial distribution of 'dummy residues' representing the protein structure. The result of the GASBOR analysis, reported in Figure 4, shows an elongated prolate shape ($\chi^2$ 0.73) that closely resembles the butterfly-shaped CK2 holoenzyme, with a good matching between the GASBOR model and the experimental atomic structure. This is the first time that the overall architecture of the $\alpha_2\beta_2$ tetrameric holoenzyme as seen in the crystalline state has been confirmed in solution.

SAXS analysis of the peak front at 0.35 M NaCl (Table 1 and Supplementary Table S2) confirms the prevalence of the monomeric form in solution. However, a higher fraction of oligomeric species (≈16% in volume) is present, most probably dimers and circular trimers that, among those with a low $\chi^2$, show the best accordance in the $R_G$ value (53.4 vs experimental 53.2 Å) (Figure 3).

SEC elution at 0.25 M salt again gives rise to an asymmetric peak (Supplementary Figure S5) that has been analysed in the front and in the tail regions. The front corresponds to a MW of 349.6 kDa and an $R_G$ value of 73.8 Å (Table 1 and Supplementary Table S3), roughly corresponding to a trimer of tetramers, $(\alpha_2\beta_2)_3$, in accordance with SEC and DLS data. The $R_G/R_S$ ratio is 0.90, indicative of an elongated shape. However, the CRYSOL fitting of the experimental diffraction curve with single models of circular or linear trimers is poor, as well as those using the dimer and the linear tetramer (Supplementary Table S3). The fitting considerably improved using mixtures of the components (using OLIGOMER), the best one being composed by 28.0% monomer, 30.5% circular trimer, 19.0% linear trimer and 22.4% linear tetramer, with $\chi^2$ 0.81 and $R_G$ 73.9 Å (Table 1 and Supplementary Table S3; Figure 5). It is notable that the dimer is scarcely or even not present in solution. Similar results are obtained with the tail of the 0.25 mM peak, with the difference that the equilibrium is now more shifted towards the monomer, which increases from 28 to 45% in volume (Table 1 and Supplementary Table S4; Figure 5). Again the fitting of different mixtures does not reveal the presence of appreciable amount of dimer. Taken together, SAXS data at 0.25 mM NaCl indicate the presence of an

**Table 1 Main SAXS results**

| **SAXS data – 0.35 M Tail** | | | $D_{max}$ (Å) | $R_G$ (Å) | MW (kDa) |
|---|---|---|---|---|---|
| | | | 180.7 | 51.7 | 128.9 |
| Fittings | Species | $\chi^2$ | % vol | $R_G$ (Å) | MW (kDa) |
| Crysol | Monomer | 0.80 | 100 | 46.87 | 130 |
| Oligomer | Mono/oligomers | 0.75 | ≈95/≈5 | ≈50 | ≈141 |
| **SAXS data – 0.35 M Front** | | | $D_{max}$ (Å) | $R_G$ (Å) | MW (kDa) |
| | | | 186.2 | 53.2 | 149.3 |
| Fittings | Species | $\chi^2$ | % vol | $R_G$ (Å) | MW (kDa) |
| Crysol | Monomer | 6.29 | 100 | 46.87 | 130 |
| Oligomer | Mono/Dim/cTri | 0.83 | 83.9/9.1/7.0 | 53.4 | 160.0 |
| **SAXS data – 0.25 M Front** | | | $D_{max}$ (Å) | $R_G$ (Å) | MW (kDa) |
| | | | 260.8 | 73.8 | 349.6 |
| Fittings | Species | $\chi^2$ | % vol | $R_G$ (Å) | MW (kDa) |
| Crysol | lTrimer | 2.01 | 100 | 81.00 | 390 |
| Oligomer | Mono/cTri/lTri/lTetra | 0.81 | 28.0/30.5/19.0/22.4 | 73.9 | 345.0 |
| **SAXS data – 0.25 M Tail** | | | $D_{max}$ (Å) | $R_G$ (Å) | MW (kDa) |
| | | | 230.7 | 68.8 | 281.1 |
| Fittings | Species | $\chi^2$ | % vol | $R_G$ (Å) | MW (kDa) |
| Crysol | Dimer | 1.74 | 100 | 63.38 | 260 |
| Oligomer | Mono/cTri/lTri/lTetra | 0.67 | 45.4/24.1/16.0/14.4 | 70.7 | 289.1 |

equilibrium in solution between different species, mainly the monomer, the linear and circular trimers and the linear tetramer, with the absence of the dimer.

SAXS data were also collected at 0.20 mM NaCl but in this case the presence of large and not homogeneous aggregates deteriorated the signal to such an extent that we could not perform reliable fittings with CRYSOL and OLIGOMER. However we could have an estimate of the average $R_G$, 139 Å, and the mean MW, around 800 kDa (Supplementary Table S5), value not far from that obtained by SEC at the same ionic strength (900 kDa). As shown in Supplementary Table S5, these values are close to those of a hexamer, but the poor quality of the SAXS signal indeed suggests the presence of a complex equilibrium between many oligomeric species.

# Discussion

Currently the prevalent model for the regulation of CK2 is based on the existence of inactive oligomers of the $\alpha_2\beta_2$ holoenzyme that, when needed, can dissociate into the monomeric active form responsible for the correct catalytic activity that triggers the physiological event. Oligomeric forms of CK2 have been described several times at values of ionic strengths near the physiological one, and evidences of the existence of aggregated CK2 in cells have been reported. Oligomerization is driven by electrostatic interactions between the catalytic and the regulatory subunits, hence the CK2 holoenzyme is usually studied at high salt, typically 0.5 M NaCl, to avoid the formation of undesirable aggregates. Circular and linear molecular models for CK2 oligomers have been proposed on the basis of crystal structures [14,16,37]. Recently, CK2 oligomerization has been investigated by native mass spectrometry, supporting the existence of both circular trimers and linear oligomers [25].

In the present study we have characterized the oligomerization process by different biophysical techniques, i.e. by SEC, DLS and in particular by SAXS, a technique that can give structural information not only on the size but, most importantly, on the shape of the complexes in solution. In studying aggregation phenomena, it is crucial to distinguish between specific and unspecific events, and often the quality of the sample is the primary determinant for the reliability of the results. We then took great care in the preparation of the samples. For the assembly of the tetrameric $\alpha_2\beta_2$ holoenzyme, the independently produced $\alpha^{(1-336)}$ and β (full sequence) subunits were mixed together and then purified by SEC at 0.35 M NaCl from possible intermediate components

Biochemical Journal (2017) **0** 1–12
DOI: 10.1042/BCJ20170189

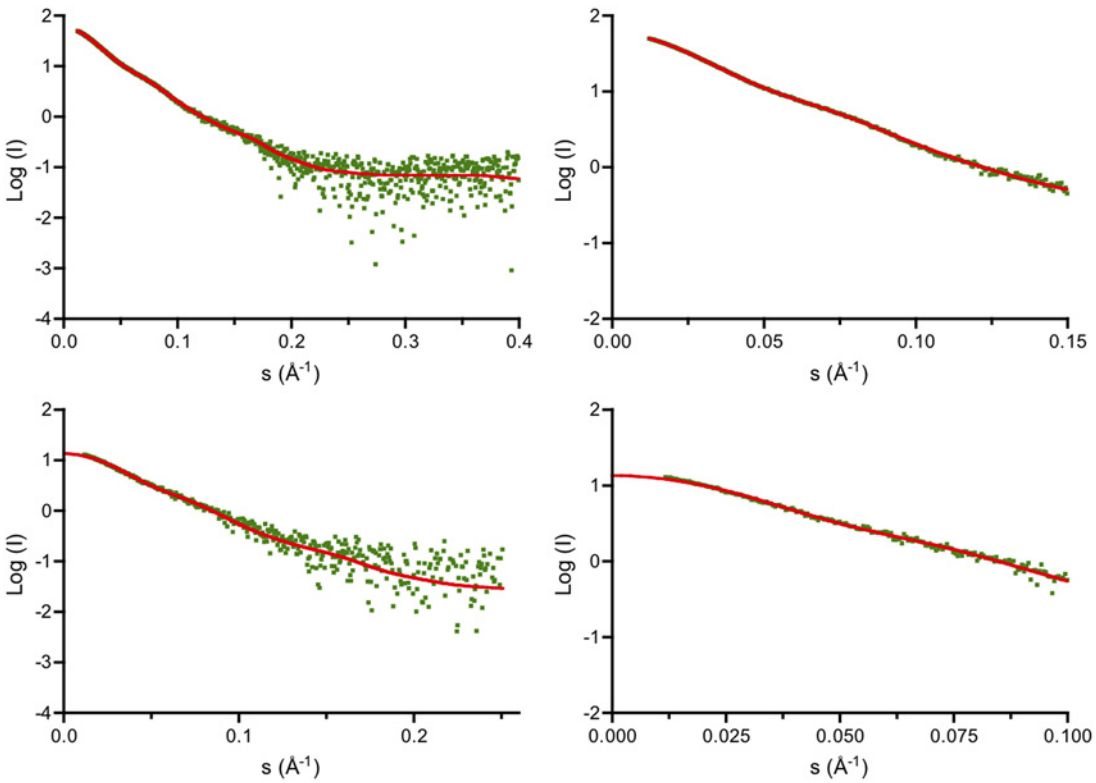


**Figure 3. Fittings of the SAXS profiles at 0.35 M NaCl.**

Upper panels: fitting by 'Oligomer' of the SEC peak front scattering profile (in green) with a mixture Mono/Dim/cTri = 83.9/9.1/7.0% (in red), $\chi^2 = 0.83$. Lower panels: fitting by 'Crysol' of the SEC peak tail scattering profile (in green) with the monomeric CK2 holoenzyme (in red), $\chi^2 = 0.80$. Right-hand panels, fittings at very low scattering angle, up to the momentum transfer s = 0.15 and 0.1 Å$^{-1}$. See also Table 1 showing SAXS results.

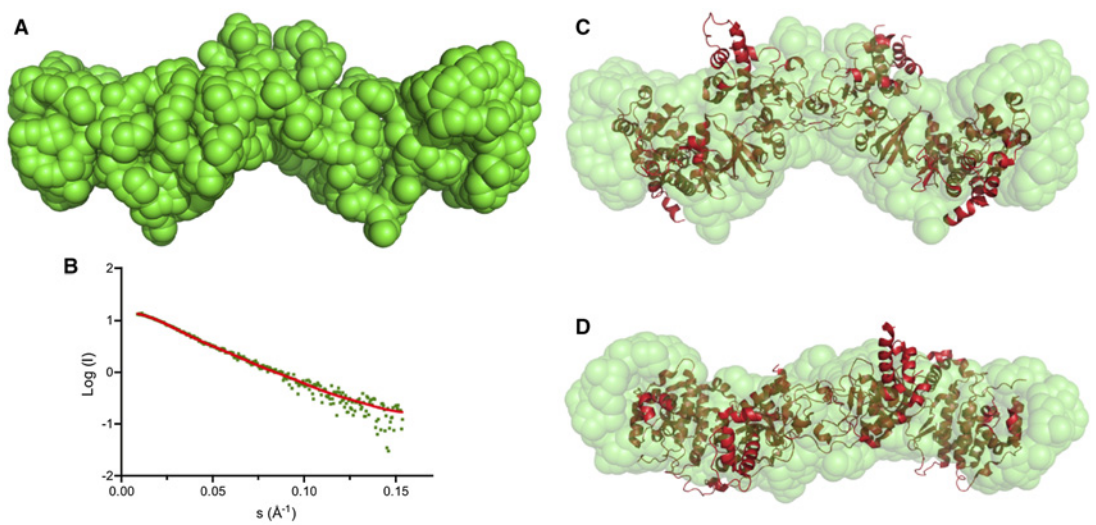


**Figure 4. Structure model generated by Gasbor using the SAXS scattering profile at 0.35 M NaCl.**

(**A**) *Ab initio* 'dummy atom' model. (**B**) Gasbor fitting (red) to the experimental data (green), $\chi^2$ 0.73. (**C**) Superposition of the *ab initio* model (in green) and the crystal structure of the CK2 holoenzyme (in red). (**D**) 90° downward rotated superposition.

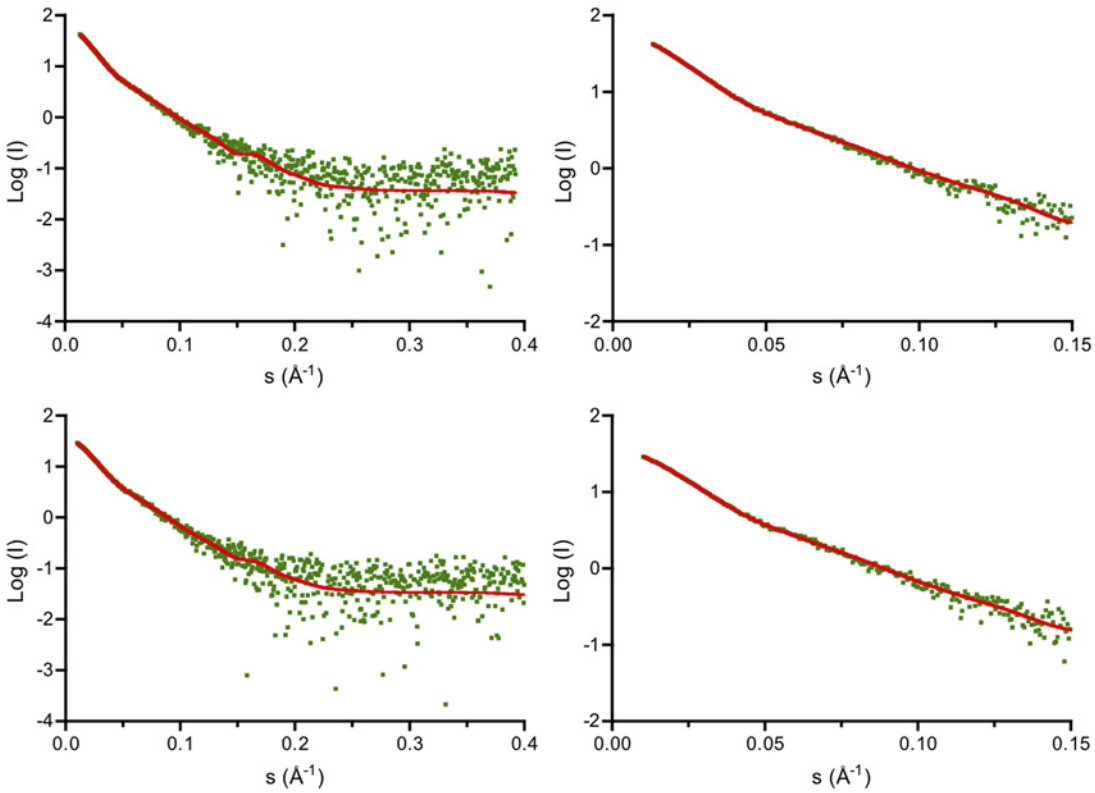


**Figure 5. SAXS fittings at 0.25 M NaCl.**

Upper panels: 'Oligomer' fitting of the SEC peak front scattering profile (in green) with a mixture Mono/cTri/lTri/lTetra = 28.0/30.5/19.0/22.4% (in red), $\chi^2 = 0.81$. Lower panels: 'Oligomer' fitting of the SEC peak tail scattering profile (in green) with the mixture Mono/cTri/lTri/lTetra = 45.4/24.1/16.0/14.4% (in red), $\chi^2 = 0.67$. Right-hand panels: fittings at very low scattering angle, up to the momentum transfer s = 0.15 Å$^{-1}$. See also Table 1 showing SAXS results.

such as $\alpha\beta_2$ and isolated $\alpha$ or $\beta_2$. This is an important point that distinguishes the present study to that using native mass spectrometry where excesses of $\alpha$ or $\beta$ were intentionally used [25]. Further, small-angle diffraction experiments in solution were performed using the SEC-SAXS configuration, where a second SEC step is immediately preceding in-line the diffraction measurement, allowing the characterization of different portions of the elution peak and of the interconverting equilibria between the single species present in solution. According to previous SEC runs (data not shown), 0.35 M is the lowest NaCl concentration that guarantees the presence of the holoenzyme essentially in the monomeric form (confirmed by succeeding SAXS results). This was assessed to minimize the background (higher at high salt) and the sample dilution for SAXS measurements at 0.25 and 0.20 M salt, so as to obtain the best possible signal-to-noise ratio.

SEC results confirmed what already was known from the literature: lowering the salt concentration induces CK2 oligomerization. In addition, using a calibrated SEC column we could estimate the molecular weight of these oligomers at 0.25 M salt, which turned out to be compatible with the presence of trimeric forms in solution, at least in their mean properties. This result was confirmed by measurements of the hydrodynamic (Stokes) radius by DLS. These oligomeric forms are stabilized by electrostatic interactions, as indicated by the capability of polybasic spermine to dissociate the trimers at 0.25 M NaCl and even the more aggregated species observed at 0.2 M NaCl. To assess the appropriateness of the oligomeric models deduced from the hexagonal and monoclinic crystal packings of the holoenzyme, we used mutated forms of the basic P + 1 loop of CK2$\alpha$ and the CK2$\beta$ acidic loop and, according to SEC, as expected the holoenzyme remains monomeric at 0.25 M salt, confirming that these regions are involved in oligomerization. The impairment in the formation of oligomers caused by a different set of mutations in the CK2$\beta$ acidic loop has been similarly reported elsewhere [25]. The residues mutated in the $\alpha$-subunit, namely Arg191, Arg195 and Lys198, are also involved in substrate

Biochemical Journal (2017) **0** 1–12
DOI: 10.1042/BCJ20170189

recruitment and, accordingly, the mutated CK2α showed a significant decrease in activity, both when isolated and in complex with the β-subunit [24]. In the same paper it was interestingly found that the holoenzyme with a β-subunit carrying the same mutations studied in the present paper and able to dissociate the oligomers, i.e. with β(noacid), is more active than the wild-type holoenzyme. This makes a clear link between the aggregation state and the catalytic capacity, supports the model of the inactivation upon oligomerization and substantiates the functional significance of the oligomeric structures as derived from crystallographic analyses.

SEC-SAXS measurements confirmed these outcomes and were also able to define the shape of the monomeric holoenzyme in solution and to detail its oligomerization equilibria. At 0.35 M NaCl, the monomer is the most abundant species in solution, between 84% and 95% in volume, and its shape, as determined by *ab-initio* procedures performed by GASBOR, i.e. without any *a priori* structural assumption, fully matches the butterfly-shaped holoenzyme seen in the crystal structures. Our SAXS data do not indicate the presence of dissociation species such as $\alpha\beta_2$, α or $\beta_2$, implying that, once correctly formed, the $\alpha_2\beta_2$ holoenzyme is 'stable' in solution. The stability of the holoenzyme as specified in the present study argues against its transient nature hypothesized in Seetoh et al. [25], where diverse 'intermediate' species $(\alpha\beta_2)_n$ were identified by native mass spectrometry. It has to be noted that firstly in native MS experiments, a truncated form of β, lacking a few residues involved in the interaction with the α-subunit, is employed; secondly, samples were prepared simply by mixing the two subunits, without any further purification step, with excesses of either α or β. Hence the detection of 'intermediate' species does not necessary imply that they are coming from the dissociation of the pre-formed tetramer. For instance, the species $\alpha\beta_2$ was identified only in presence of an excess of β and not in the case of an excess of α, suggesting that it could also be a consequence of the unbalanced stoichiometry rather than of the dissociation of the $\alpha_2\beta_2$ holoenzyme. Instead, SAXS data presented here show that, once formed and carefully isolated from components in excess, the tetrameric form of the holoenzyme is stable and does not spontaneously dissociate in solution, in accordance with the $K_d$ of approximately 5÷10 nM determined by ITC. This is in agreement with a similar conclusion derived by the detailed analysis of the α/β interfaces in the symmetric holoenzyme (PDB ID 4MD7) [15], and is supported by the jsPISA assembly stock analysis [38] of the same crystal structure indicating that the most probable oligomeric state with the maximum aggregation index is the $\alpha_2\beta_2$ tetramer, with the absence of partial assemblies such as $\alpha\beta_2$. The presence of $\alpha\beta_2$ is predicted by jsPISA when analysing the asymmetric enzyme (PDB ID 4DGL or 1JWH) that indeed is present only in the circular trimers, where other stabilizing contributions come from inter-tetrameric interactions. Interestingly however, the presence of the intermediate $\alpha\beta_2$ in excess of $\beta_2$, as shown by native MS and confirmed by our SEC experiments (data not shown), indicates the lack of any positive allostery in the formation of $\alpha_2\beta_2$, i.e. the two recruitment sites in $\beta_2$ are equal and independent. This is in accordance with ITC binding data [39], showing only one sharp transition at the 2:1 $\alpha$:$\beta_2$ stoichiometry, and with the presence of two identical α/β interfaces in the symmetric structure of the holoenzyme when not involved in cyclic trimers [15].

At 0.25 M salt, the 'average properties' [MW, $R_G$ and maximum particle size ($D_{max}$)] determined by SAXS are compatible with a trimeric CK2, as determined by other techniques like SEC and DLS that give as output only one single average quantity (MW or $R_S$). However, fittings of the experimental profiles with molecular models show that indeed several species are present in solution, the most probable being a mixture of monomer, circular trimer, linear trimer and linear tetramer. Of particular interest is the finding of an unexpected considerable amount of monomer at 0.25 M salt despite the average properties of a trimer.

Overall data presented here further support the model of CK2 regulation by auto-inhibitory oligomerization. In solution the monomeric $\alpha_2\beta_2$ holoenzyme is in equilibrium both with circular trimers and linear oligomers such as dimers, trimers, tetramers, etc. At 0.35 M NaCl, both equilibria are shifted towards the monomer, the largely prevailing species, while at 0.25 M NaCl comparable amounts of circular trimers on one hand and linear trimers and tetramers on the other are present, as well as a relevant amount of the monomer itself (Supplementary Figure S6). Regarding the question of which aggregated form is physiologically more relevant, we notice that the closed, circular trimer, with a three-fold symmetry axis, is structurally favoured by the positive cooperativity in the formation of the three equal interfaces (versus the two independent interfaces of the linear assembly) [15]. This is in accordance with recently uncovered evolutionary evidences that establish preferences for the existence of rotational symmetry-related regular oligomers over non-symmetric ones [40].

PORTLAND PRESS

## Author Contribution

G.L. and R.B. designed the study, collected SAXS data and analyzed results; G.L. and D.N. prepared the samples and performed SEC and DLS analyses; S.S. provided CK2 mutants. R.B. analyzed SAXS data and wrote the paper.

## Q5 Funding

Q6 This work was supported by funds from the Department of Chemical Sciences and from the University of Padua (Progetto Giovani) [GRIC101044] (to G.L.).

## Acknowledgements

The authors thank the staff of BM29 BioSAXS beamline at ESRF Grenoble (F) for on-site assistance in data collection.

## Q7 Competing Interests

Q8 The authors declare that there are no competing interests associated with the manuscript.

## Abbreviations

DLS, dynamic light scattering; $D_{max}$, maximum particle size; ESRF, European Synchrotron Radiation Facility $R_G$, radius of gyration; $R_S$, Stokes radius; SAXS, small angle X-ray scattering; SEC, size-exclusion chromatography.

# References

1 Pinna, L.A. (ed.) (2013) *Protein Kinase CK2*. Wiley-Blackwell, Oxford, U.K
2 Ruzzene, M. and Pinna, L.A. (2010) Addiction to protein kinase CK2: a common denominator of diverse cancer cells? *Biochim. Biophys. Acta, Proteins Proteomics* **1804**, 499–504 doi:10.1016/j.bbapap.2009.07.018
3 Guerra, B. and Issinger, O.-G. (2008) Protein kinase CK2 in human diseases. *Curr. Med. Chem.* **15**, 1870–1886 doi:10.2174/092986708785132933
4 Rabalski, A.J., Gyenis, L. and Litchfield, D.W. (2016) Molecular pathways: emergence of protein kinase CK2 (CSNK2) as a potential target to inhibit survival and DNA damage response and repair pathways in cancer cells. *Clin. Cancer Res.* **22**, 2840–2847 doi:10.1158/1078-0432.CCR-15-1314
5 Battistutta, R. (2009) Protein kinase CK2 in health and disease: structural bases of protein kinase CK2 inhibition. *Cell. Mol. Life Sci.* **66**, 1868–1889 doi:10.1007/s00018-009-9155-x
6 Battistutta, R., Cozza, G., Pierre, F., Papinutto, E., Lolli, G., Sarno, S. et al. (2011) Unprecedented selectivity and structural determinants of a new class of protein kinase CK2 inhibitors in clinical trials for the treatment of cancer. *Biochemistry* **50**, 8478–8488 doi:10.1021/bi2008382
7 Cozza, G., Girardi, C., Ranchio, A., Lolli, G., Sarno, S., Orzeszko, A. et al. (2014) Cell-permeable dual inhibitors of protein kinases CK2 and PIM-1: structural features and pharmacological potential. *Cell. Mol. Life Sci.* **71**, 3173–3185 doi:10.1007/s00018-013-1552-5
8 Lolli, G., Cozza, G., Mazzorana, M., Tibaldi, E., Cesaro, L., Donella-Deana, A. et al. (2012) Inhibition of protein kinase CK2 by flavonoids and tyrphostins. A structural insight. *Biochemistry* **51**, 6097–6107 doi:10.1021/bi300531c
9 Sarno, S., Papinutto, E., Franchin, C., Bain, J., Elliott, M., Meggio, F. et al. (2011) ATP site-directed inhibitors of protein kinase CK2: an update. *Curr. Top. Med. Chem.* **11**, 1340–1351 doi:10.2174/156802611795589638
10 Niefind, K. and Battistutta, R. (2013) Structural bases of protein kinase CK2 function and inhibition. In *Protein Kinase CK2* (Pinna, L.A., ed.), pp. 3–75, Wiley-Blackwell, Oxford, U.K
11 Battistutta, R. and Lolli, G. (2011) Structural and functional determinants of protein kinase CK2α: facts and open questions. *Mol. Cell. Biochem.* **356**, 67–73 doi:10.1007/s11010-011-0939-6
12 Papinutto, E., Ranchio, A., Lolli, G., Pinna, L.A. and Battistutta, R. (2012) Structural and functional analysis of the flexible regions of the catalytic α-subunit of protein kinase CK2. *J. Struct. Biol.* **177**, 382–391 doi:10.1016/j.jsb.2011.12.007
13 Niefind, K., Guerra, B., Ermakowa, I. and Issinger, O.-G. (2001) Crystal structure of human protein kinase CK2: insights into basic properties of the CK2 holoenzyme. *EMBO J.* **20**, 5320–5331 doi:10.1093/emboj/20.19.5320
14 Lolli, G., Pinna, L.A. and Battistutta, R. (2012) Structural determinants of protein kinase CK2 regulation by autoinhibitory polymerization. *ACS Chem. Biol.* **7**, 1158–1163 doi:10.1021/cb300054n
15 Lolli, G., Ranchio, A. and Battistutta, R. (2014) Active form of the protein kinase CK2 $\alpha_2\beta_2$ holoenzyme is a strong complex with symmetric architecture. *ACS Chem. Biol.* **9**, 366–371 doi:10.1021/cb400771y
16 Schnitzler, A., Olsen, B.B., Issinger, O.-G. and Niefind, K. (2014) The protein kinase $CK2^{Andante}$ holoenzyme structure supports proposed models of autoregulation and trans-autophosphorylation. *J. Mol. Biol.* **426**, 1871–1882 doi:10.1016/j.jmb.2014.02.018
17 Glover, C.V. (1986) A filamentous form of Drosophila casein kinase II. *J. Biol. Chem.* **261**, 14349–14354 PMID:3095319
18 Poole, A., Poore, T., Bandhakavi, S., McCann, R.O., Hanna, D.E. and Glover, C.V.C. (2005) A global view of CK2 function and regulation. *Mol. Cell. Biochem.* **274**, 163–170 doi:10.1007/s11010-005-2945-z
19 Valero, E., De Bonis, S., Filhol, O., Wade, R.H., Langowski, J., Chambaz, E.M. et al. (1995) Quaternary structure of casein kinase 2. characterization of multiple oligomeric states and relation with its catalytic activity. *J. Biol. Chem.* **270**, 8345–8352 doi:10.1074/jbc.270.14.8345
20 Filhol, O., Nueda, A., Martel, V., Gerber-Scokaert, D., Benitez, M.J., Souchier, C. et al. (2003) Live-cell fluorescence imaging reveals the dynamics of protein kinase CK2 individual subunits. *Mol. Cell. Biol.* **23**, 975–987 doi:10.1128/MCB.23.3.975-987.2003
21 Theis-Febvre, N., Martel, V., Laudet, B., Souchier, C., Grunwald, D., Cochet, C. et al. (2005) Highlighting protein kinase CK2 movement in living cells. *Mol. Cell. Biochem.* **274**, 15–22 doi:10.1007/s11010-005-3115-z

Biochemical Journal (2017) **0** 1–12
DOI: 10.1042/BCJ20170189

22 Hübner, G.M., Larsen, J.N., Guerra, B., Niefind, K., Vrecl, M. and Issinger, O.G. (2014) Evidence for aggregation of protein kinase CK2 in the cell: a novel strategy for studying CK2 holoenzyme interaction by BRET$^2$. *Mol. Cell. Biochem.* **397**, 285–293 doi:10.1007/s11010-014-2196-y
23 Boldyreff, B., Meggio, F., Pinna, L.A. and Issinger, O.G. (1993) Reconstitution of normal and hyperactivated forms of casein kinase-2 by variably mutated β-subunits. *Biochemistry* **32**, 12672–12677 doi:10.1021/bi00210a016
24 Sarno, S., Vaglio, P., Marin, O., Meggio, F., Issinger, O.-G. and Pinna, L.A. (1997) Basic residues in the 74-83 and 191-198 segments of protein kinase CK2 catalytic subunit are implicated in negative but not in positive regulation by the β-subunit. *Eur. J. Biochem.* **248**, 290–295 doi:10.1111/j.1432-1033.1997.00290.x
25 Seetoh, W.-G., Chan, D.S.-H., Matak-Vinković, D. and Abell, C. (2016) Mass spectrometry reveals protein kinase CK2 high-order oligomerization via the circular and linear assembly. *ACS Chem. Biol.* **11**, 1511–1517 doi:10.1021/acschembio.6b00064
26 Pernot, P., Round, A., Barrett, R., De Maria Antolinos, A., Gobbo, A., Gordon, E. et al. (2013) Upgraded ESRF BM29 beamline for SAXS on macromolecules in solution. *J. Synchrotron Radiat.* **20**, 660–664 doi:10.1107/S0909049513010431
27 Round, A., Brown, E., Marcellin, R., Kapp, U., Westfall, C.S., Jez, J.M. et al. (2013) Determination of the GH3.12 protein conformation through HPLC-integrated SAXS measurements combined with X-ray crystallography. *Acta Crystallogr. D Biol. Crystallogr.* **69**, 2072–2080 doi:10.1107/S0907444913019276
28 Brennich, M.E., Kieffer, J., Bonamis, G., De Maria Antolinos, A., Hutin, S., Pernot, P. et al. (2016) Online data analysis at the ESRF BioSAXS beamline. *J. Appl. Cryst.* **49**, 203–212 doi:10.1107/S1600576715024462
29 De Maria Antolinos, A., Pernot, P., Brennich, M.E., Kieffer, J., Bowler, M.W., Delageniere, S. et al. (2015) ISPyb for BioSAXS, the gateway to user autonomy in solution scattering experiments. *Acta Crystallogr. D Biol. Crystallogr.* **71**, 76–85 doi:10.1107/S1399004714019609
30 Rambo, R.P. and Tainer, J.A. (2013) Accurate assessment of mass, models and resolution by small-angle scattering. *Nature* **496**, 477–481 doi:10.1038/nature12070
31 Konarev, P.V., Volkov, V.V., Sokolova, A.V., Koch, M.H.J. and Svergun, D.I. (2003) *PRIMUS*: a Windows PC-based system for small-angle scattering data analysis. *J. Appl. Cryst.* **36**, 1277–1282 doi:10.1107/S0021889803012779
32 Petoukhov, M.V., Franke, D., Shkumatov, A.V., Tria, G., Kikhney, A.G., Gajda, M. et al. (2012) New developments in the *ATSAS* program package for small-angle scattering data analysis. *J. Appl. Cryst.* **45**, 342–350 doi:10.1107/S0021889812007662
33 Konarev, P.V. and Svergun, D.I. (2015) *A posteriori* determination of the useful data range for small-angle scattering experiments on dilute monodisperse systems. *IUCrJ* **2**, 352–360 doi:10.1107/S2052252515005163
34 Svergun, D.I., Barberato, C. and Koch, M.H.J. (1995) *CRYSOL* – a program to evaluate x-ray solution scattering of biological macromolecules from atomic coordinates. *J. Appl. Cryst.* **28**, 768–773 doi:10.1107/S0021889895007047
35 Svergun, D.I., Petoukhov, M.V. and Koch, M.H.J. (2001) Determination of domain structure of proteins from X-ray solution scattering. *Biophys J.* **80**, 2946–2953 doi:10.1016/S0006-3495(01)76260-1
36 Cochet, C. and Chambaz, E.M. (1983) Polyamine-mediated protein phosphorylations: a possible target for intracellular polyamine action. *Mol. Cell. Endocrinol.* **30**, 247–266 doi:10.1016/0303-7207(83)90062-X
37 Niefind, K. and Issinger, O.-G. (2005) Primary and secondary interactions between CK2α and CK2β lead to ring-like structures in the crystals of the CK2 holoenzyme. *Mol. Cell. Biochem.* **274**, 3–14 doi:10.1007/s11010-005-3114-0
38 Krissinel, E. (2015) Stock-based detection of protein oligomeric states in jsPISA. *Nucleic Acids Res.* **43**, W314–W319 doi:10.1093/nar/gkv314
39 Raaf, J., Bischoff, N., Klopffleisch, K., Brunstein, E., Olsen, B.B., Vilk, G. et al. (2011) Interaction between CK2α and CK2β, the subunits of protein kinase CK2: thermodynamic contributions of key residues on the CK2α surface. *Biochemistry* **50**, 512–522 doi:10.1021/bi1013563
40 Ahnert, S.E., Marsh, J.A., Hernandez, H., Robinson, C.V. and Teichmann, S.A. (2015) Principles of assembly reveal a periodic table of protein complexes. *Science* **350**, aaa2245 doi:10.1126/science.aaa2245